www.czasopisma.pan.pl PAN POLSKA AKADEMIA NAUK www.journals.pan.pl

Arch. Min. Sci. **71** (2026), 1, 103-122

Electronic version (in color) of this paper is available: http://mining.archives.pl

DOI: https://doi.org/10.24425/ams.2026.157758

JIAN ZHAO[1*], DAN HUANG[1], ZHIJIE ZHENG[1], GUANGZHE ZHANG[2], MIN ZHANG[3]

EXPERIMENTAL AND NUMERICAL INVESTIGATIONS ON ROCK CUTTABILITY USING CONICAL PICKS CUTTING: A CASE STUDY IN A PHOSPHATE MINE

To investigate the rock cuttability in a phosphate mine in China, conventional rock mechanical tests and rock indentation tests were conducted on specimens sampled from five different rock layers. Rock strength parameters and maximum rock cutting forces were determined. Subsequently, numerical simulation was employed to further investigate the rock cuttability of the selected rock specimen through the rock linear cutting test. Unlike rock indentation tests, which determine only the maximum rock cutting force based on a single cutting cycle, numerical simulations can enable the determination of the maximum cutting force, average cutting force and specific energy (SE). The numerical simulation results for the maximum rock cutting force showed a good agreement with the experimental results after calibrating the numerical model and parameters. The results indicate that the rock strength of the Chuanyandong Phosphate Mine ranges from 21 MPa to 145 MPa. The maximum cutting force ranges from 0.85 kN to 2.88 kN, with an average value of 1.93 kN. The SE of ore body b is 10 kWh/m^3. Additionally, the numerical simulation shows that the volume of rock cutting fragments increases linearly with the cutting displacement, and there is a significant influence of cutting velocity on the simulated rock cutting performance. Finally, the rock cuttability of the phosphate mine was classified based on rock strengths, cutting forces, SE and instantaneous cutting rate (ICR) predictions. In general, the rock cuttability improves with the decrease of rock strength, cutting force and SE, while the increase of ICR.

Keywords: Rock cuttability; Rock indentation test; Rock linear cutting test; Rock fragment volume; Numerical simulation

[1] INSTITUTE OF MINING ENGINEERING, BGRIMM TECHNOLOGY GROUP, NO. 22 BEIXING ROAD EAST, DAXING DISTRICT, BEIJING 102628, PR CHINA
[2] INSTITUTE OF FOUNDATION ENGINEERING, CHINA ACADEMY OF BUILDING RESEARCH, NO. 30 BEISANHUAN EAST ROAD, CHAOYANG DISTRICT, BEIJING 100013, PR CHINA
[3] GEOTECHNICAL INSTITUTE, TU BERGAKADEMIE FREIBERG, GUSTAV-ZEUNER-STRABE 1, FREIBERG 09599, GERMANY

* Corresponding author: zhaojian@bgrimm.com

1. Introduction

Rock cuttability is a comprehensive index that reflects the difficulty of interaction between mechanical cutting tools and rock materials [1-3]. Its classification is mainly used to assess the feasibility of using a cantilever roadheader for excavating roadways and tunnels [4]. The cuttability level is influenced by many factors, including the rock mechanical properties [5,6], the rock confining stress [7,8], the geometric parameters of conical picks [9] and the cutting parameters [10]. With the increasing demand for mechanical excavation in civil and mining engineering, a growing number of researchers are studying rock cutting through experiments and numerical simulations [11] to optimise the cutting process and improve cutting efficiency.

Experimental research on rock cuttability is the most fundamental and reliable method for assessing rock cuttability, including conventional rock mechanical experiments and rock cutting experiments [12]. The conventional mechanical test measures rock properties such as UCS and tensile strength, while the rock cutting test evaluates the cutting force of a conical pick and the specific energy (SE) [13,14]. There are two scales of rock cutting tests: full-scale rock cutting tests and core sample-based cuttability tests. Full-scale rock cutting tests more closely reproduce the actual rock cutting conditions and do not suffer from the scaling effect. However, their disadvantages include being labour-intensive, time-consuming and expensive [15]. Thus, the rock cutting test generally refers to the core sample-based cuttability test and is commonly conducted using a linear cutting machine (LCM). For instance, Wang et al. [16] investigated the relationship between peak cutting force and uniaxial confining stress using cuboid hard rock samples of 300×120×120 mm, and Wicaksana et al. [17] performed a linear cutting test using sandstone rocks with a trimmed size of 300×300×200 mm to study the rock cutting process taking account of the dynamic loading at intermediate strain rate. And Comakli et al. [18] accomplished small-scale linear cutting tests using core samples from eight different metallic ores in Turkey, to predict the performance of roadheaders in metallic ore excavation via the SE. In addition to the LCM, Luo and Qiao [19] introduced a small-scale rotary cutting machine (RCM) to study both cutting force and radial resistance, and Liu [20] also designed the RCM-based test bed to measure the cutting force when cutting coal and rock using a drum with about 20 picks. And to predict the SE using rock brittleness in rock cutting, Raghavan and Murthy [21] studied the influence of the attack angle and pick angle on the SE, where the rock specimen is 0.3×0.3×0.45 m, and the cutter head is a drum that has 12 picks. Furthermore, the rock specimen of the rotary cutting test by Zhang et al. [22] reached 1.2×0.8×0.6 m, and they found that the rock fracture is dominated by tensile failure, accompanied by squeezing and shearing failure, through collecting and analysing the shape, colour, and block size of caved rock fragments. However, it is still difficult to detect the rock fracture propagation experimentally, as well as for the rock failure process in the cutting process [23], which is helpful to utilise the original rock flaws, such as cracks, to improve the cutting efficiency.

The numerical simulation approach has been taken as an easier and faster method to predict the rock cutting performance in the last decade, including finite element method (FEM), discrete element method (DEM) and hybrid method [24]. At present, there has been a lot of research showing that DEM is more capable of reproducing the failure formation and the crack distribution [25,26]. According to the document by Jiang and Meng [27], FEM typically uses element erosion to approximate the rock failure, while DEM often uses rigid discs or spheres to approximate the rock micro-structure. In recent efforts, Wang et al. [28] and Lu et al. [29] studied the cracks of

arc rock plate forming in the rock cutting process using the finite element software ANSYS/LS-DYNA, and they concluded that the cutting velocity has an unobvious influence on the mean peak cutting force. Jeong et al. [30] replicated similar cutter forces, SE and fragmentation phenomenon as the experimental results using the smooth particle hydrodynamics (SPH) simulation technique, which is a mesh-free Lagrangian method. Apart from the FEM, a 2D discrete element modelling (DEM) rock cutting model was established by Zhang et al. [31] to analyse the rock breaking and cutting force, and they found that the particle diameter in the DEM model has an obvious effect on the macro-mechanical parameters of the rock model. What's more, they also mentioned that it is necessary to correct the cutting velocity of the DEM using laboratory experiments during the rock cutting calculation.

Based on the research overview above, conducting rock linear cutting tests requires large rock samples, while numerical simulations of these tests rarely count the volume of rock cutting fragments and subsequently calculate the specific energy. Moreover, there is very little literature analysing the classification of rock cuttability. In this study, to evaluate the feasibility of non-blasting mechanical excavation of a roadway using a cantilever roadheader in a phosphate mine in China, experimental research was first conducted. This research included an experimental investigation of the conventional rock mechanical properties and the rock cutting performance using a conical pick. Then, a DEM-based numerical model of rock cutting was set up using PFC3D to investigate fracture propagation and rock breaking performance, aiming to better understand the rock cutting process. Finally, a comprehensive analysis of rock cuttability was implemented, and the excavation efficiency was predicted. The research process is illustrated in Fig. 1.

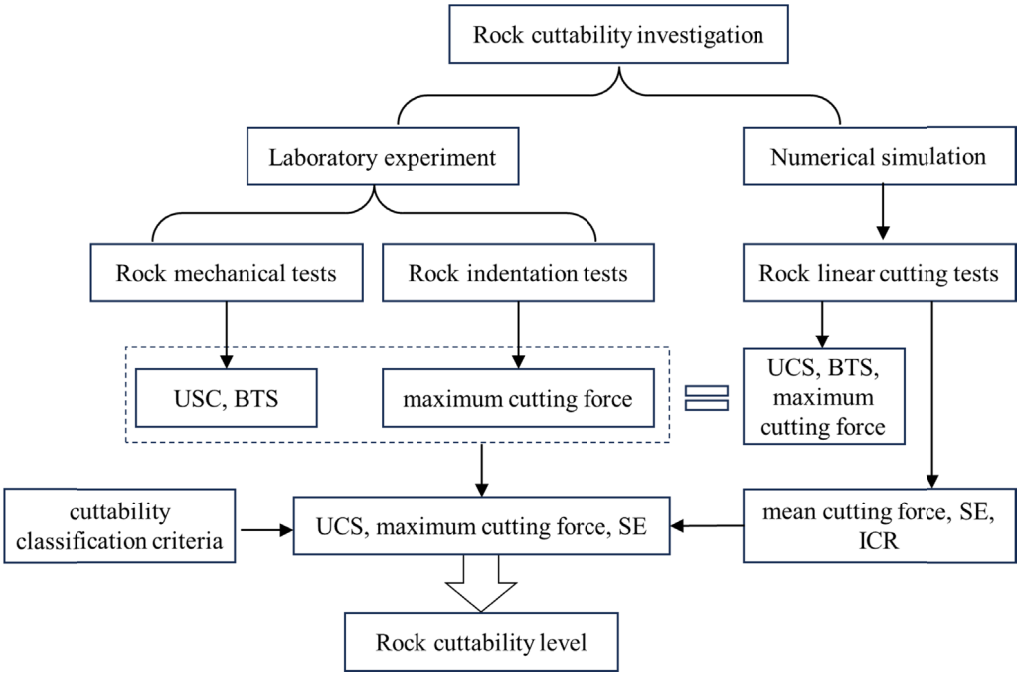

Fig. 1. Rock Cuttability investigation flowchart through rock indentation test and numerical simulation

2. Experimental procedure and results

2.1. Rock specimen and mechanical test

The Chuanyandong Phosphate Mine, located in Guizhou Province, China, is owned by Wengfu Group Co., Ltd. Fig. 2 presents the ore body deposits and the layout profile of the development roadway. To assess the feasibility of mechanical excavation using a cantilever roadheader and to enhance the economy and efficiency of roadway excavation, it is essential to investigate the conventional mechanical properties of the rock specimens and the linear cutting performance.

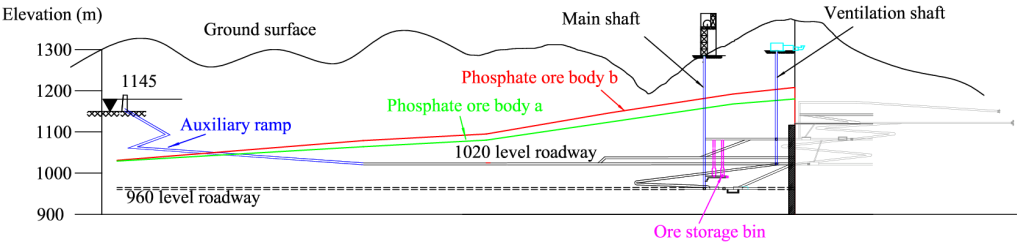

Fig. 2. Development system of the Chuanyandong Phosphate Mine

The rock specimens were sampled from various layers of the phosphate mine, including phosphate ore body a, phosphate ore body b, the roof layer bU of phosphate ore body b, the floor layer aD of phosphate ore body a, as well as the interlayer (bD) between the two phosphate ore bodies. Fig. 3 and TABLE 1 provide detailed information on rock sampling, specimen process-

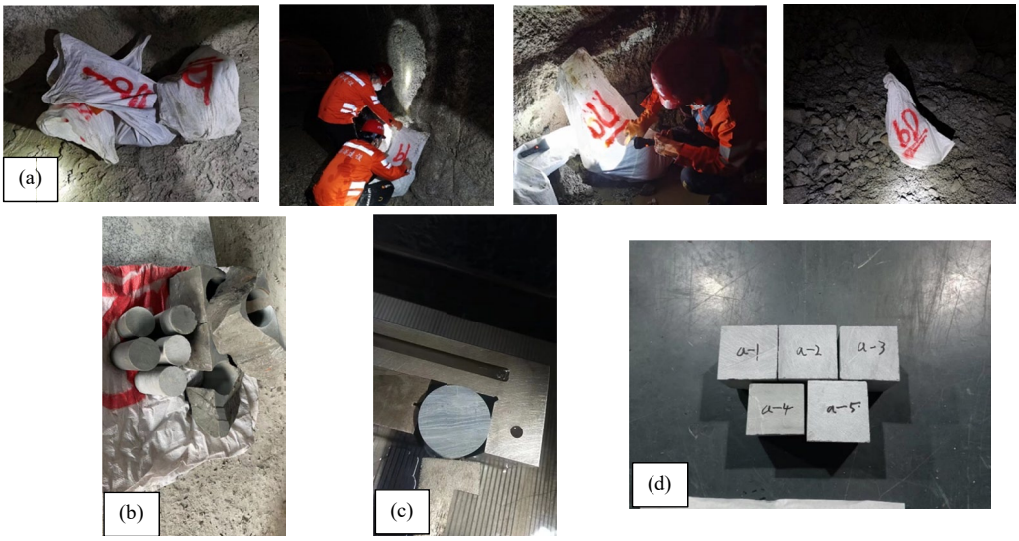

Fig. 3. Rock sampling and specimen processing at the Chuanyandong Phosphate Mine: (a) Rock sampling, (b) Cylindrical specimen, (c) Brazilian disk specimen, (d) Cubic specimen

ing and rock specimen characteristics. The rock specimens conform to the standard sample sizes and include cylindrical specimens with a diameter of 50 mm and a height of 100 mm, as shown in Fig. 3(b), and the Brazilian disk specimens with a diameter of 50 mm and a height of 25 mm, as shown in Fig. 3(c). The cubic specimens with a side length of 60 mm, used for rock indentation tests, are shown in Fig. 3(d).

TABLE 1

Rock specimen information

Rock layer symbol	Rock layer position	Thickness (m)	Lithology	Sampling method
bU	Roof of ore body b	16.92~42.88	Grey and light grey thick micrite dolomite	Massive rock
b	Phosphate ore body b	9.49~28.93 (16.27 on average)	Dolomitic phosphate rock	Massive rock
bD	Interlayer	10.66~11.95	Light grey thick micrite dolomite	Massive rock
a	Phosphate ore body a	17.45~35.32 (27.16 on average)	Dolomitic phosphate rock	Massive rock
aD	Floor of ore body a	0~53.40	Sage green clay dolomite	Massive rock

The field investigation results of the rockmass joints are given in TABLE 2. It can be observed that the joints in the rockmass located in the ore body a and its floor aD belong to the middle spacing joints. In contrast, the ore body b exhibits dense spacing joints, while the roof layer bU and the interlayer bD display very dense spacing joint. Moreover, the joints in the ore body a and b are humid, and those in the roof of ore body b and the interlayer bD are dry. Water seepage occurs in the floor layer aD.

TABLE 2

Rockmass joint investigation results

Rock layer symbol	Joint number	Length of scan line (m)	Average spacing (mm)	Spacing level	Water permeability
bU	21	1	48	Very dense	Dry
b	226	30	133	Dense	Humid
	66		455	Middle	
bD	250	10	40	Very dense	Dry
	20		500	Middle	
a	66	30	455	Middle	Humid
	40		750	Loose	
aD	84	30	357	Middle	Seepage

The rock uniaxial compression and Brazilian splitting tests were conducted using the compression test machine, as presented in Fig. 4(a). The triaxial compression test machine, depicted in Fig. 4 (b), was adopted to measure and calculate the rock's cohesion and friction angle.

The UCS, tensile strength, cohesion and friction angle can be calculated from conventional mechanical tests through equations (1) to (4) [32,33]. Here, UCS represents the uniaxial com-

Fig. 4. Conventional rock mechanical test machines: (a) Compression test machine, (b) Triaxial compression test machine

pressive strength; P_{max} is the maximum load applied to the specimen; A is the cross-sectional area of the specimen; σ_t is the tensile strength; D is the specimen diameter; H is the specimen height; φ is the friction angle; k is the slope of the relationship curve between σ_1 and σ_3, where σ_1 and σ_3 denote maximum loading stress and confining stress respectively; c is the cohesion; σ_0 is the y-intercept of the relationship curve between σ_1 and σ_3.

$$UCS = \frac{P_{max}}{A} \tag{1}$$

$$\sigma_t = \frac{2P_{max}}{\pi DH} \tag{2}$$

$$\varphi = \arcsin\frac{k-1}{k+1} \tag{3}$$

$$c = \sigma_0 \frac{(1-\sin\varphi)}{2\cos\varphi} \tag{4}$$

2.2. Rock indentation test

Fig. 5(a) exhibits a typical cutting force evolution during a continuous linear cutting test using the LCM, which comprises multiple cutting cycles. In each cycle, the cutting force firstly drops to a lower value after large rock chips are separated, then gradually increases until the next chip separation. The LCM is a widely accepted experimental method for assessing rock cutting performance. Its advantages include relatively simple equipment, low construction costs, and suitability for studying the effects of cutting parameters on cutting force and SE [34,35].

However, the linear cutting test using the LCM requires a larger rock specimen compared to conventional rock mechanical tests. Hence, some researchers have adopted the rock indentation test to investigate the rock cutting performance [36,37], as it requires a smaller rock specimen. This test involves only a single cutting cycle, specifically the process from the conical pick contacting the rock specimen to the separation of the rock chip. Fig. 5(b) presents the rock indentation machine used in this study. The conical pick indents into the rock at a location 9 mm away from the edge of the rock sample.

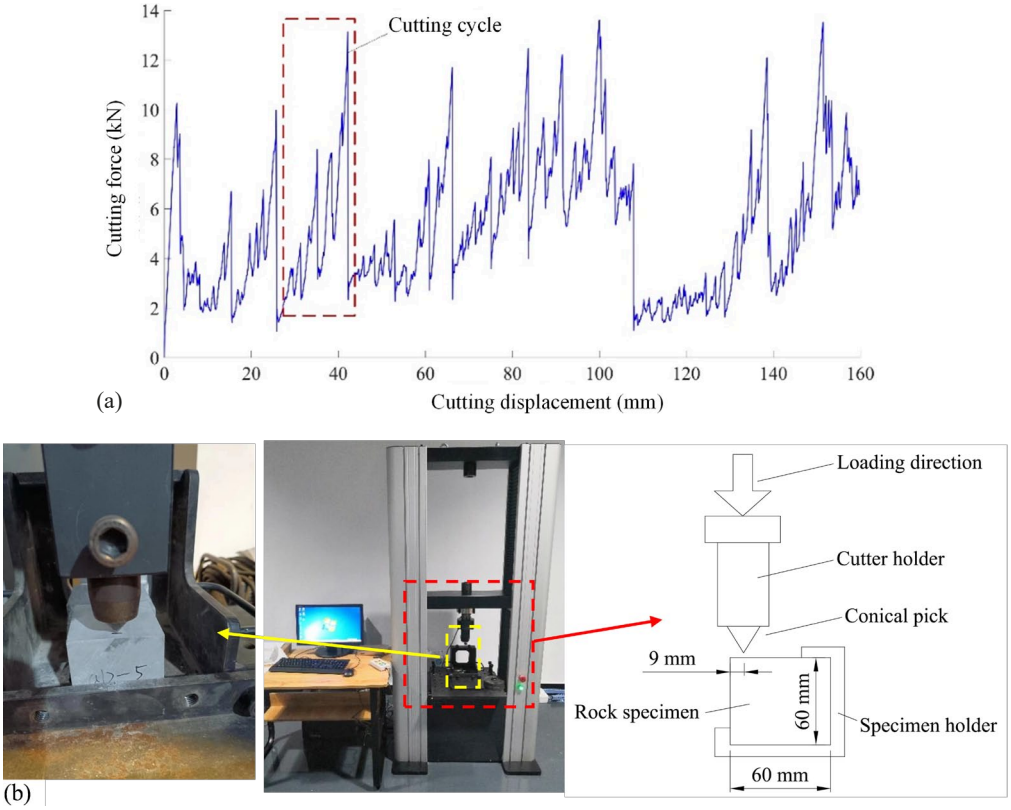

Fig. 5. Rock indentation test: (a) Typical cutting force evolution using the LCM, (b) Rock indentation machine

According to the experimental procedure and recommendations documented by Huang et al. [38], the attack angle is set to 0°. To minimise the influence of the rock specimen variability on the experimental results, five rock indentation tests should be conducted on the rock specimens from the same rock layers mentioned in TABLE 1. The maximum and mean cutting forces are evaluated by the curve depicting the relationship between cutting force and cutting displacement, and the SE is calculated using Eq. (5), where F_c represents the mean cutting force, l is the cutting displacement, and V is the volume of rock cut [39].

$$SE = F_c l / V \tag{5}$$

2.3. Conventional mechanical properties

The experimental results of conventional rock mechanical properties are listed in TABLE 3. They show that the elastic modulus and the UCS are generally low, due to the well-developed primary fissures, as documented in TABLE 2. In addition, mechanical deformation and strength properties experience a huge reduction after being fully saturated due to the softening coefficient, particularly in the ore bodies a, b and their interlayer bD. These factors, lower rock strength, well-developed primary fissures, and water-induced softening, facilitate the rock cutting using a conical pick. Therefore, it is preliminarily feasible to adopt a mechanical mining method using a cantilever roadheader at the Chuanyandong Phosphate Mine, based on the evaluation of the conventional rock mechanical test data.

Nevertheless, these data can't be directly used as the micro-property parameters for the DEM-based numerical model. It is necessary to calibrate the micro-properties to match the measured mechanical properties through modelling the uniaxial compressive strength test and Brazilian tensile strength test [40].

TABLE 3

Physical and mechanical properties of rock specimens from the Chuanyandong Phosphate Mine

Rock layer symbol	ρ (g/cm^3)	σ_c (MPa)	E (GPa)	v	k	σ_t (MPa)	c (MPa)	φ (°)
bU	2.75	45.37	7.50	0.21	0.91	4.63	7.25	54.57
b	2.75	21.35	3.10	0.22	0.77	4.13	4.70	42.52
bD	2.74	28.95	3.60	0.23	0.66	4.74	5.86	45.94
a	2.74	72.61	8.50	0.28	0.70	11.21	14.26	47.10
aD	2.76	144.68	76.24	0.13	0.91	8.08	16.28	63.4

ρ – density; σ_c – uniaxial compressive strength; E – elastic modulus; v – Poisson's ratio; k – softening coefficient; σ_t – tensile strength; c – cohesion; φ – friction angle.

2.4. Rock cutting force

Fig. 6 shows the evolution of cutting force versus cutting displacement, and the cutting force statistics are summarised in TABLE 4. These results illustrate that the maximum cutting force is about 2 kN on average. In addition, the mean cutting force and the SE are not available for the rock indentation test due to only a single cutting cycle. This limitation can be addressed through linear cutting tests or corresponding numerical simulations.

TABLE 4

Cutting force of rock specimens from the Chuanyandong Phosphate Mine

Rock layer symbol	Specimen symbol	F_{max} (kN)	$\bar{F}_{max}$ (kN)
1	2	3	4
bU	bU-1	2.41	2.22
	bU-2	2.75	
	bU-3	2.11	
	bU-4	1.48	
	bU-5	2.37	

TABLE 4. Continued

1	2	3	4
b	b-1	1.95	1.47
	b-2	1.36	
	b-3	1.00	
	b-4	2.18	
	b-5	0.85	
bD	bD-1	0.94	1.85
	bD-2	2.88	
	bD-3	1.14	
	bD-4	2.52	
	bD-5	1.76	
a	a-1	1.71	1.86
	a-2	2.37	
	a-3	1.49	
	a-4	1.15	
	a-5	2.56	
aD	aD-1	1.86	2.23
	aD-2	2.57	
	aD-3	2.67	
	aD-4	1.25	
	aD-5	2.80	

F_{max} – max. cutting force; $\bar{F}_{max}$ – average of max. cutting force.

On the other hand, the experimental investigation results regarding rock cutting force are based on the unconfined state, making this a preliminary study for assessing rock cuttability. Further study could focus on rock cutting efficiency under different rock flaw situations and confining stress scenarios.

3. Numerical simulation of rock linear cutting test: A case of ore body b

3.1. Numerical model set-up

It is feasible to obtain rock mechanical properties and cutting performance parameters through experimental investigations, such as rock indentation tests, to assess the cuttability of phosphate rock. But the fracture propagation and rock breaking performance are still unclear. In this context, the rock linear cutting process is simulated using discontinuum-based numerical modelling. PFC3D is a widely used discrete element method (DEM) software, where a numerical model consists of rigid ball or block elements connected by contact elements. Initially, the ball or block elements are bonded by these contact elements, and cracks appear following the failure of the contact elements.

This study selects the rock specimen of the phosphate ore body b as a case study for numerical simulation. The micro-property parameters of the numerical model are first calibrated

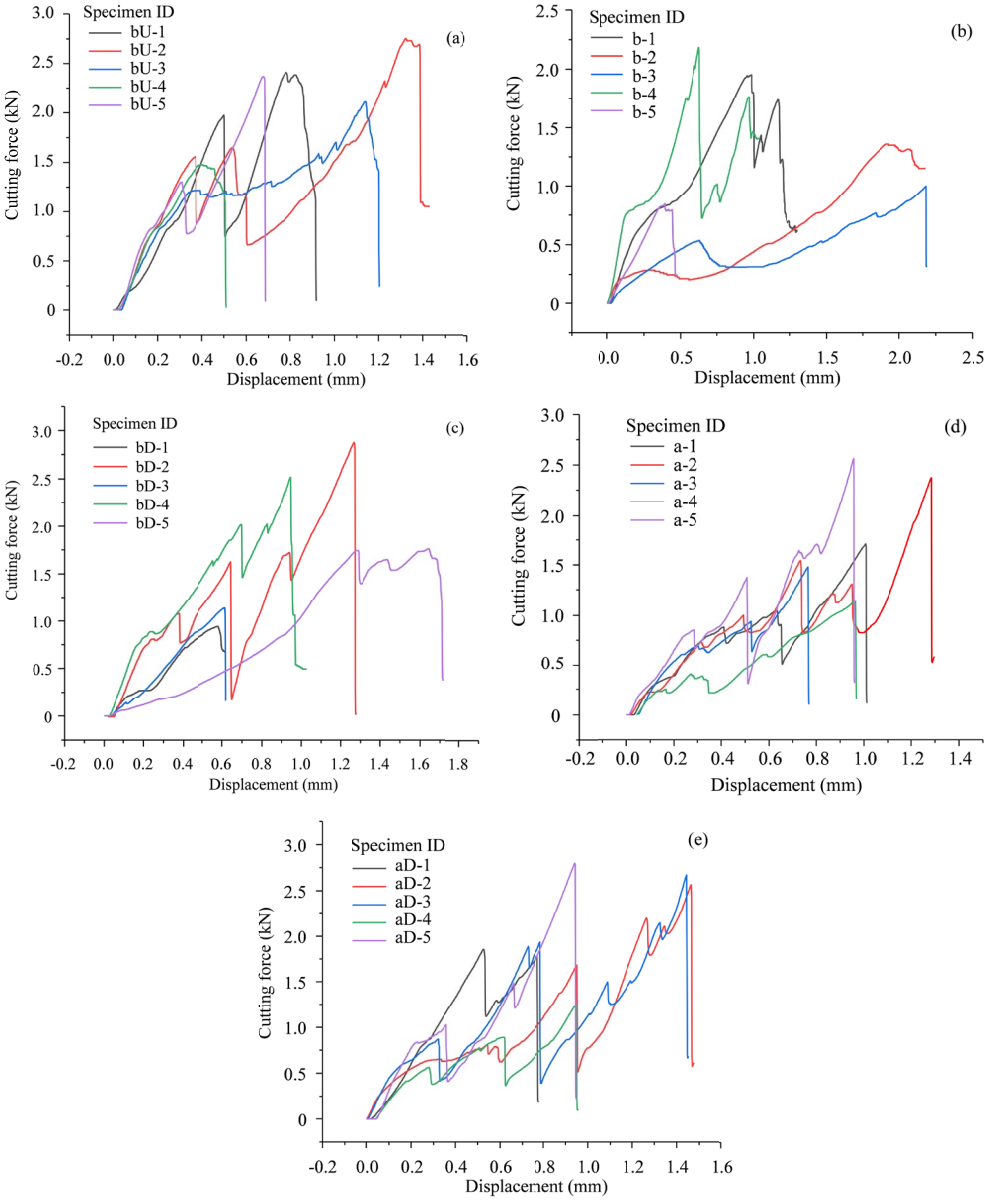

Fig. 6. Cutting force evolution of 5 rock specimens over cutting displacement at each rock layer position: (a)-(e) stand for the rock specimens from rock layers bU, b, bD, a and aD

using uniaxial compressive strength (UCS) and Brazilian tensile strength (BTS) tests. The soft-bond model is adopted for the contact material model of the rock sample, which is represented by block elements [41], with the relevant model parameters shown in TABLE 5. The contact model between the conical pick (wall element) and the rock sample (block element) is a linear

model. The numerical models of the rock samples adopt Voronoi block elements. Different from conventional numerical simulations of rock cutting, which are modelled by spherical blocks, Voronoi block elements have varied particle shapes that better represent the irregular shapes of mineral particles in crystalline rocks such as phosphate rock. Fig. 7 gives a comparison of the macro-properties between laboratory tests and numerical simulations. The results are consistent with the laboratory data mentioned in TABLE 3, confirming that simulated macro-mechanical response corresponds to the micro-mechanical parameters listed in TABLE 5. The simulated UCS and BTS values are calculated by Eq. (1) and Eq. (2), respectively.

TABLE 5

Micro-properties of phosphate ore body b

Property	Block	Bond contact
d (mm)	0.5	—
ρ (kg/m^3)	2740	—
μ		0.2
E (GPa)		3.0
k_n / ks		2.0
φ (°)		20°
c (MPa)		11
σ_t (MPa)		7

E – effective modulus; d – average geometric size; ρ – density; μ – friction coefficient; k_n / ks – normal-to-shear stiffness ratio; φ – friction angle; c – cohesion; σ_t – tensile strength.

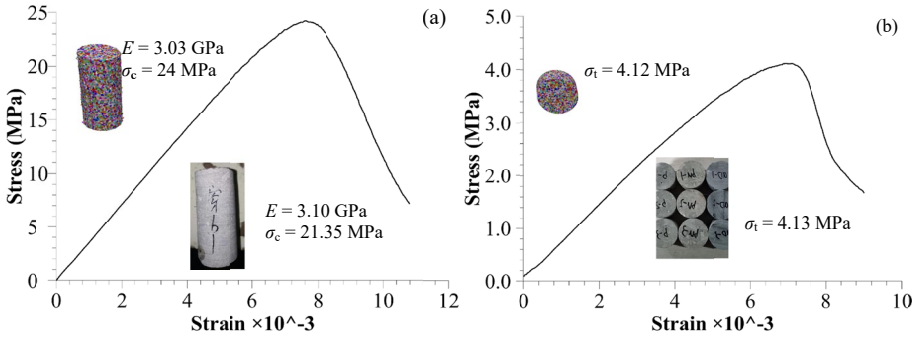

Fig. 7. Comparison of Macro-properties phosphate rock specimen b between laboratory tests and numerical simulations: (a) UCS simulation test, (b) BTS simulation test

After calibration, a rock linear cutting numerical model is set up to investigate rock cutting performance, as shown in Fig. 7. To accelerate the calculations, the model dimensions are set to 40×40×20 mm, with an average Voronoi block size of 0.5 mm around the cutting area. There are around 71,066 blocks. The bottom boundary of the numerical model is fixed, while all other model surfaces are free boundaries. The conical pick has a tip angle of 80°, identical to that used in the rock indentation test. The attack angle is set to 90° to make sure that the conical pick is perpendicular to the rock surface, consistent with the rock indentation tests. The attack angle,

like other cutting parameters, significantly influences cutting performances, warranting further sensitivity analysis in future studies. The cutting velocity is maintained at a constant 1 m/s, with a cutting depth of 2 mm. A cutting displacement of 20 mm is applied to ensure a stable long-term cutting stage and multiple cutting cycles.

During the numerical simulation of the rock linear cutting test, the cutting forces acting on the conical pick are monitored by recording the contact forces between the conical pick and the rock blocks, including the normal force, cutting force and sideway force. The volume of cut rock is obtained by summing the volumes of rock fragments. Subsequently, the SE is calculated by Eq. (5) based on the numerical simulation results. Specifically, the cut rock volume is determined by collecting and summing the volume of each rock fragment generated during the linear cutting, utilising the FISH function in PFC3D. In addition, the bond breakages are tracked in the numerical model to simulate crack initiation and fracture propagation within the rock specimen.

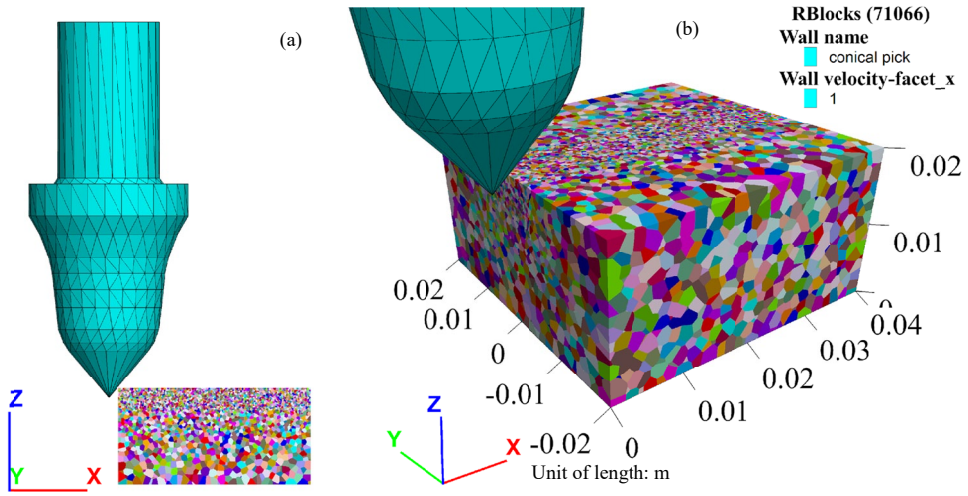

Fig. 8. Numerical model of rock linear cutting. (a) Front view; (b) Overall view

3.2. Simulation results

Based on the simulation results, the cutting force evolutions in the three directions are illustrated in Fig. 8. It is obvious that the maximum cutting forces over multiple cutting cycles vary from 0.6 kN to 2.2 kN, with an average maximum cutting force of about 1.5 kN. This value is identical to the laboratory results for the rock specimen b, as documented in Fig. 6(b) and TABLE 4. The estimated mean cutting forces are about 0.80 kN for both the cutting force and the normal force, and –0.03 kN for the sideways force. Besides, the variation in cutting force with respect to cutting displacement is highly consistent with the normal force. Given that the tip angle is 80°, this results in a half tip angle of 40°. This angle is close to 45°, allowing the force acting on the pick tip surface to be decomposed into two approximately equal component forces.

When the conical pick touches the micro block particles of the rock specimen numerical model, the bonded contacts gradually break, leading to the formation of micro-cracks. As the

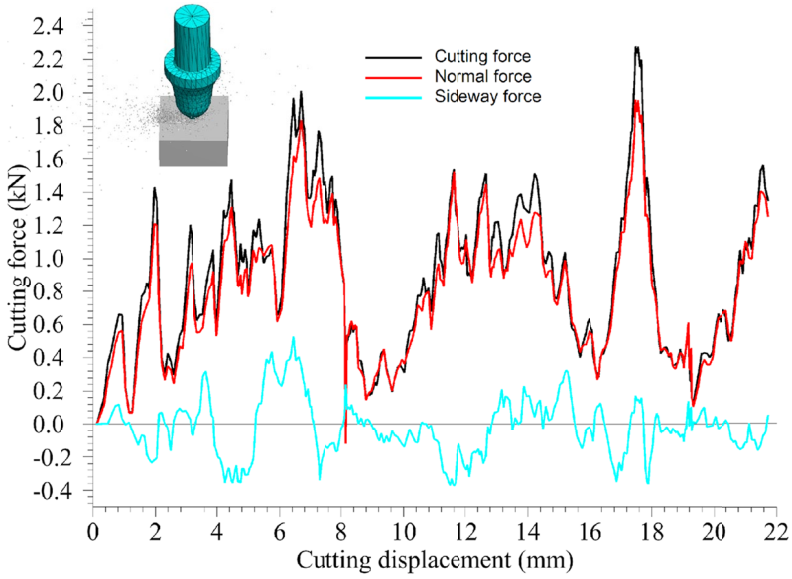

Fig. 9. Cutting force evolution in the numerical simulation of rock linear cutting

number of cracks increases, these micro-cracks propagate into macro-fractures, resulting in the formation of rock chips and fragments [42]. The fracture distribution during linear cutting is shown in Fig. 10, and the rock fragments are presented in Fig. 11. The variation in rock fragment volume with cutting displacement is described in Fig. 11.

Fig. 10 indicates that rock breaking is primarily caused by the tensile failure of bonded microscopic blocks, and the extent of rock crack propagation is larger than that of the rock fragments. What's more, it is also tensile failure that causes micro-fracture to propagate into the intact rock during rock cutting. In Fig. 10, it is evident that the formation of rock fragments or chips primarily depends on the micro-block elements of the numerical model. Most of the fragment volumes correspond to individual micro-blocks, although some larger fragments consist of multiple micro-blocks.

The total volume of rock fragments, that is, the volume of cut rock, increases linearly with the cutting displacement, as shown in Fig. 12. From Fig. 12, it can also be seen that the cut rock volume corresponding to a cutting displacement of 20 mm is about 0.42 cm^3. By substituting this value into Eq. (5), the SE calculated from the simulation results is about 10 kWh/m^3.

Based on the simulated SE, the cutting performance of roadheaders in ore body b can be forecasted. A performance prediction model for roadheaders is proposed by Rostami et al. [43], and the instantaneous cutting rate (ICR) of the roadheader is calculated approximately using the following equation.

$$ICR = \frac{kP}{SE} \tag{6}$$

Where, k is the energy transfer ratio, usually assumed to be 0.8 for a roadheader [18]; P is the cutting head power.

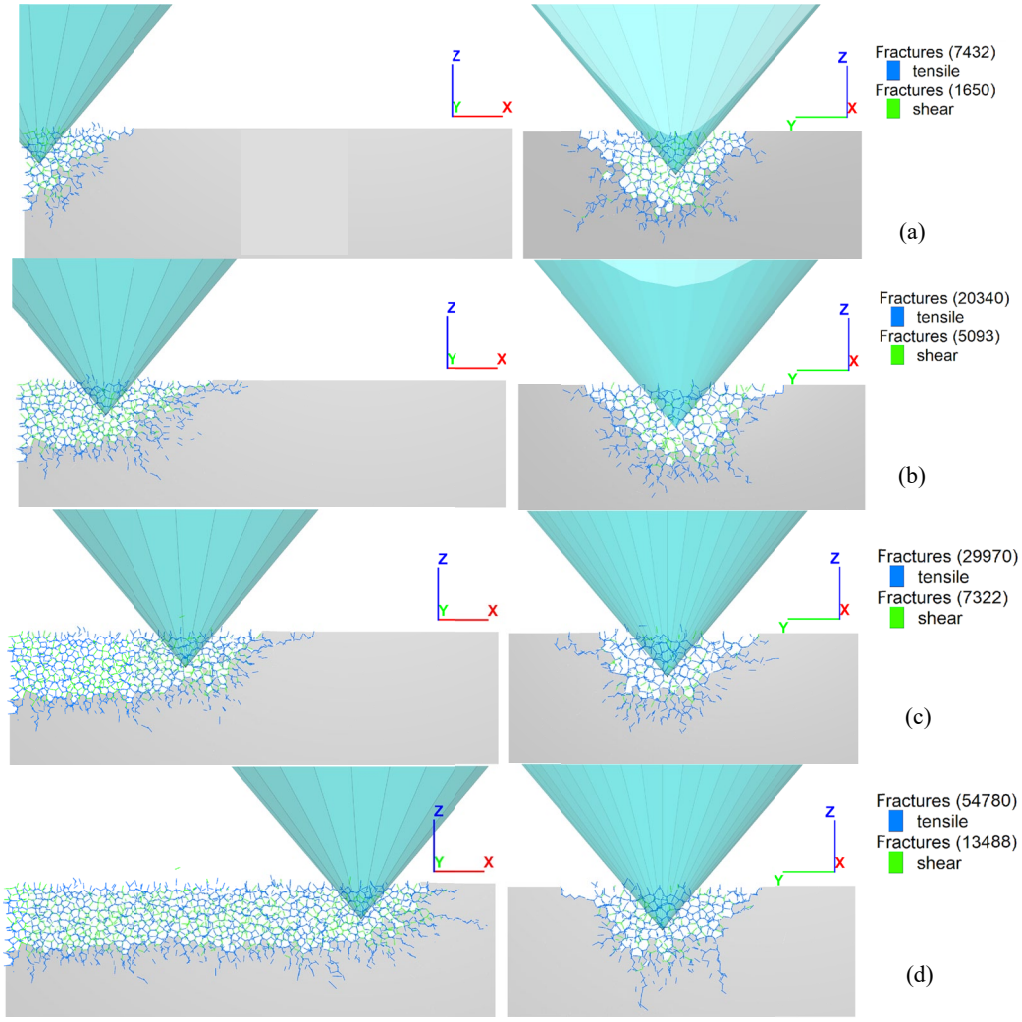

Fig. 10. Fracture evolution with cutting displacement, blue line stands for tensile crack, green line for shear crack: (a) 1 mm cutting displacement, (b) 5 mm, (c) 10 mm, (d) 20 mm

Taking a roadheader with a cutting power of 200 kW as an example, the corresponding predicted cutting rate is about ICR = 0.8 × 200 / 10 = 16 m^3/h.

The daily advance is about 5 m during four hours of pure mechanical excavation, corresponding to a cutting rate of 17.5 m^3/h, when using the cantilever roadheader in a roadway profile of 4 × 3.5 m at the Chuanyandong Phosphate Mine. The field industrial application results have a good agreement with the predicted ICR data calculated by the simulated SE.

Fig. 13 depicts the influence of cutting velocity on the average cutting force and the rock fragment volume, both of which are related to the SE of rock cutting. It reveals a significant effect on rock cutting performance when assigning different cutting velocities in DEM-based modelling. Therefore, it is essential to calibrate the cutting velocity of the conical pick by comparing

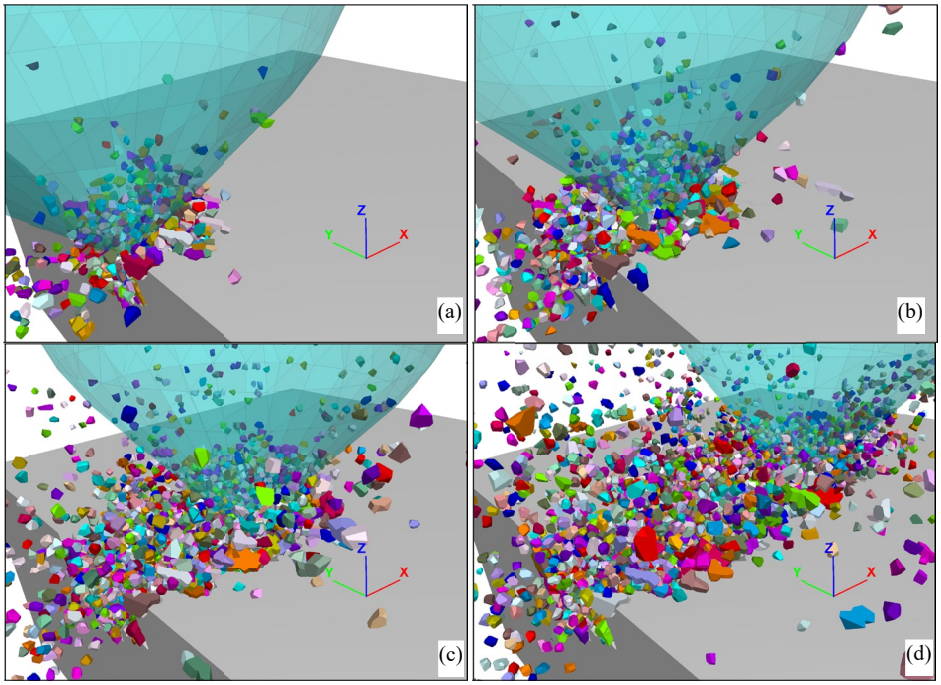

Fig. 11. Rock fragment evolution with cutting displacement: (a) 1 mm cutting displacement, (b) 5 mm, (c) 10 mm, (d) 20 mm

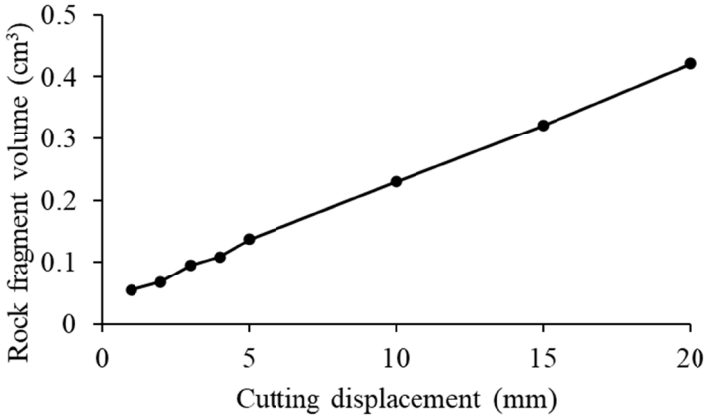

Fig. 12. Rock fragment volume variation with cutting displacement

laboratory results with numerical simulations. In this study, the cutting velocity was calibrated by comparing the cutting forces obtained from experiments and numerical simulations. Specifically, a simulated cutting velocity of 1 m/s ensured good agreement between the experimental and numerical results.

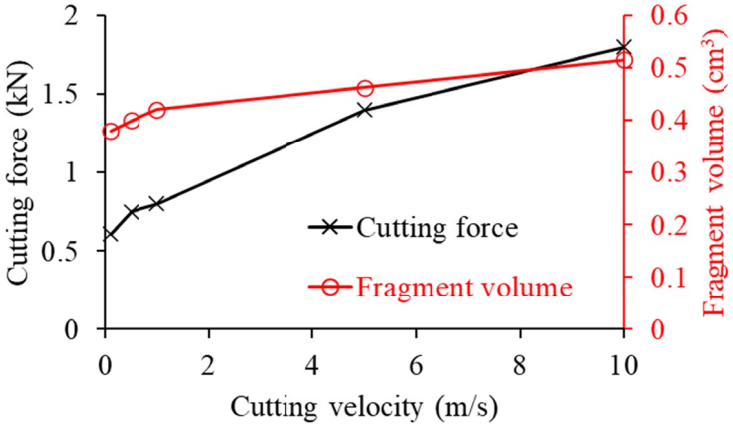

Fig. 13. Influence of cutting velocity on rock cutting simulation results

4. Rock cuttability discussion

4.1. Investigation method comparison

Two experimental investigation methods, the rock indentation test and the rock linear cutting test, are compared in TABLE 5 for assessing the cuttability of phosphate rock. Generally speaking, the linear cutting test is a better measure, because of more accurate cutting force and

TABLE 5

Comparison of investigation method of rock cuttability

Investigation method		Advantages	Disadvantages
Laboratory test	Rock indentation test	• test device and procedure are simple • test cost is low • maximum cutting force is available	• only a single cutting cycle • average cutting force and SE are not available • closer to the point load test
	Rock linear cutting test	• include multiple cutting cycles • average cutting force is available • SE is available • closer to the actual condition of conical pick • accurate cutting force • actual friction and abrasion of conical pick	• test device and procedure are complex • rock specimen is large in size • highly labor- and time-consuming • poor to investigate the micro-behaviour of rock cutting
Numerical simulation	DEM	• good repeatability and sensitivity analysis • good consistency with laboratory results • good investigation of the micro-behaviour of rock cutting	• need to calibrate the numerical model and its parameters

SE results. Nonetheless, the rock indentation test is also a feasible method for roughly evaluating rock cuttability. When the experimental equipment and budget are limited. Laboratory tests, particularly the linear cutting test, can provide more accurate cutting force and SE results, but the associated costs and labour requirements are higher. In contrast, numerical simulation can produce equally accurate cutting force and SE results after calibrating the numerical model and parameters. In addition, numerical simulations offer the convenience of investigating the micro-behaviour of rock cutting and identifying sensitive parameters that affect cutting performance.

4.2. Cuttability classification

Rock cuttability is classified to evaluate the difficulty and efficiency of rock cutting. It depends on factors such as rock cutting performance and the roadheader performance, including rock strength, rock cutting force, SE and cutting rate. By combining the mechanical properties and cutting forces mentioned in TABLES 2 to 4, along with simulation results for the ore body b, the rock cuttability for excavating roadways in different rock layers of the Chuanyandong Phosphate Mine is assessed, as shown in TABLE 6. Among these, rock layers b and bD are classified as easy to cut, rock layer bU and a as moderately easy, and rock layer aD as difficult to cut. The cuttability classification standard consists of three levels: (1) Easy to cut, $\sigma_c \leq 40$ MPa, $\overline{F}_{max} \leq 2.0$ kN, $SE \leq 5.0$ kWh/m^3, (2) Middle easy to cut, 40 MPa $< \sigma_c \leq 80$ MPa, 2.0 kN $< \overline{F}_{max} \leq 4.0$ kN, 5.0 kWh/m^3 $< SE \leq 10.0$ kWh/m^3, (3) Difficult to cut, $\sigma_c > 80$ MPa, $\overline{F}_{max} > 4.0$ kN, $SE > 10$ kWh/m^3.

TABLE 6

Cuttability classification of rock layer at the Chuanyandong Phosphate Mine

Rock layer symbol	Joint spacing level	σ_c (MPa)	σ_t (MPa)	$\overline{F}_{max}$ (kN)	SE (kWh/m^3)	ICR (m^3/h)	Cuttability
bU	Very dense	45.37	4.63	2.22	—	—	Middle
b	Middle ~ Dense	21.35	4.13	1.47	10.00	16.00	Easy
bD	Middle ~ Very dense	28.95	4.74	1.85	—	—	Easy
a	Loose ~ Middle	72.61	11.21	1.86	—	—	Middle
aD	Middle	144.68	8.08	2.23	—	—	Difficult

5. Conclusions

There is a growing demand for adopting roadheaders to excavate roadways in the mining and civil engineering industries in China, driven by continuous technological advancements. To ensure the successful application of excavation equipment and enhance excavation efficiency, it is important to assess rock cuttability. In this study, laboratory tests and DEM-based numerical simulations were employed to study the rock cuttability of five rock layers at the Chuanyandong Phosphate Mine. First, experimental investigations were conducted to determine the conventional mechanical properties of rock specimens and preliminary rock cutting performance. Next, linear cutting tests were simulated using PFC3D to reveal the micro-behaviour of rock cutting. Finally, rock cuttability was classified based on conventional mechanical properties and rock cutting

performance, specifically for the Chuanyandong Phosphate Mine. The main conclusions are drawn as follows:

(1) With respect to the conventional experimental results, the rock specimens sampled from the Chuanyandong Phosphate Mine exhibit uniaxial compressive strengths ranging from 21 MPa to 145 MPa. The average strength ratio between UCS and BTS is about 10. As for the experimental results from the rock indentation tests on five rock layers, the maximum cutting force varies from 0.85 kN to 2.88 kN, with an average of 1.93 kN.

(2) Taking the rock layer b as a case study for numerical simulation of the rock linear cutting test, the numerical model and microscopic parameters were calibrated. The results showed that the maximum cutting force for the rock layer b is about 1.5 kN, averaged over multiple cutting cycles. This simulated maximum cutting force agrees well with the experimental results. In addition, the average cutting force and normal force are about 0.80 kN and –0.03 kN for the sideways force, respectively. Also, the predicted ICR, calculated from the simulated SE shows good agreement with the in-situ excavation efficiency. Specifically, the simulated SE for the rock layer b is about 10 kWh/m^3, corresponding to an ICR of 16 m^3/h.

(3) The fragment volume during rock cutting is linearly and positively correlated with the cutting displacement when using DEM-based numerical simulation. In particular, the assigned cutting velocity of the conical pick significantly influences the cutting force and SE. As a result, the cutting velocity must be calibrated using experimental results.

(4) The assessment of rock cuttability depends on rock strength, cutting force, specific energy (SE) and instantaneous cutting rate (ICR) predictions. Generally, the rock cuttability improves with decreases in rock strength, cutting force and SE, and with an increase in ICR. Most rock layers are classified as easy or moderately easy to cut, except for the rock layer aD at the Chuanyandong Phosphate Mine.

Statement

(1) Funding: The research is supported by the National Key Research and Development Program of China (No. 2021YFC2902102, No. 2025YFE0219800).

(2) Competing Interests: The authors have no relevant financial or non-financial interests to disclose.

References

[1] N.G. Yilmaz, D. Tumac, R.M. Goktan, Rock cuttability assessment using the concept of hybrid dynamic hardness (HDH). Bull. Eng. Geol. Environ. (2015). DOI: https://doi.org/10.1007/s10064-014-0692-7

[2] A.E. Dursun, M.K. Gokay, Cuttability assessment of selected rocks through different brittleness values. Rock Mech. Rock Eng. (2016). DOI: https://doi.org/10.1007/s00603-015-0810-2

[3] O. Su, Numerical Modeling of Cuttability and Shear Behavior of Chisel Picks. Rock Mech. Rock Eng. (2019). DOI: https://doi.org/10.1007/s00603-018-1644-5

[4] S. Wang, X. Li, J. Yao, F. Gong, X. Li, K. Du, M. Tao, L. Huang, S. Du, Experimental investigation of rock breakage by a conical pick and its application to non-explosive mechanized mining in deep hard rock. Int. J. Rock Mech. Min. Sci. (2019). DOI: https://doi.org/10.1016/j.ijrmms.2019.104063

[5] S. Yasar, Predictive plots for conical pick performance using mechanical and elastoplastic properties of rocks. J. Rock Mech. Geotech. Eng. (2020). DOI: https://doi.org/10.1016/j.jrmge.2019.12.020

[6] N. Bilgin, C. Feridunoglu, D. Tumac, H. Copur, C. Balci, H. Tuncdemir, Neural networks analysis for estimating rock cuttability from rock properties. In: Proc. 41st U.S. Rock Mech. Symp. – ARMA's Golden Rocks 2006 – 50 Years Rock Mech., 2006.

[7] S. Wang, X. Li, K. Du, S. Wang, Experimental investigation of hard rock fragmentation using a conical pick on true triaxial test apparatus. Tunn. Undergr. Sp. Technol. (2018). DOI: https://doi.org/10.1016/j.tust.2018.05.006

[8] S. Wang, L. Huang, X. Li, Analysis of rockburst triggered by hard rock fragmentation using a conical pick under high uniaxial stress. Tunn. Undergr. Sp. Technol. (2020). DOI: https://doi.org/10.1016/j.tust.2019.103195

[9] G. Zhang, W. Dang, M. Herbst, Z. Song, Complex analysis of rock cutting with consideration of rock-tool interaction using distinct element method (Dem). Geomech. Eng. (2020). DOI: https://doi.org/10.12989/gae.2020.20.5.421

[10] Z. Lu, L. Wan, Q. Zeng, X. Zhang, K. Gao, Numerical Simulation of Fragment Separation during Rock Cutting Using a 3D Dynamic Finite Element Analysis Code. Adv. Mater. Sci. Eng. (2017). DOI: https://doi.org/10.1155/2017/3024918

[11] P.L. Menezes, M.R. Lovell, I.V. Avdeev, J.S. Lin, C.F. Higgs, Studies on the formation of discontinuous chips during rock cutting using an explicit finite element model. Int. J. Adv. Manuf. Technol. (2014). DOI: https://doi.org/10.1007/s00170-013-5309-y

[12] H. Kang, J.W. Cho, J.Y. Park, J.S. Jang, J.H. Kim, K.W. Kim, J. Rostami, J.W. Lee, A new linear cutting machine for assessing the rock-cutting performance of a pick cutter. Int. J. Rock Mech. Min. Sci. (2016). DOI: https://doi.org/10.1016/j.ijrmms.2016.07.021

[13] G. Zhang, H. Konietzky, T. Frühwirt, Investigation of scratching specific energy in the Cerchar abrasivity test and its application for evaluating rock-tool interaction and efficiency of rock cutting. Wear (2020). DOI: https://doi.org/10.1016/j.wear.2020.203218

[14] Y. Zhou, W. Zhang, I. Gamwo, J.S. Lin, Mechanical specific energy versus depth of cut in rock cutting and drilling. Int. J. Rock Mech. Min. Sci. (2017). DOI: https://doi.org/10.1016/j.ijrmms.2017.11.004

[15] H. Copur, N. Bilgin, H. Tuncdemir, C. Balci, A set of indices based on indentation tests for assessment of rock cutting performance and rock properties. J. South African Inst. Min. Metall. (2003).

[16] S. Wang, L. Sun, X. Li, J. Zhou, K. Du, S. Wang, M. Khandelwal, Experimental investigation and theoretical analysis of indentations on cuboid hard rock using a conical pick under uniaxial lateral stress. Geomech. Geophys. Geo-Energy Geo-Resources (2022). DOI: https://doi.org/10.1007/s40948-022-00345-x

[17] Y. Wicaksana, H. Jeong, S. Jeon, Numerical simulation of rock cutting process induced by a pick cutter considering dynamic properties of rock at intermediate strain rate. Bull. Eng. Geol. Environ. (2021). DOI: https://doi.org/10.1007/s10064-021-02471-4

[18] R. Comakli, S. Kahraman, C. Balci, Performance prediction of roadheaders in metallic ore excavation. Tunn. Undergr. Sp. Technol. (2014). DOI: https://doi.org/10.1016/j.tust.2013.09.009

[19] C. Luo, J. Qiao, J. Zhou, Z. Sun, J. Cao, Cutting mechanical study of pick cutting coal seams with coal and rock interface. Energy Reports (2022). DOI: https://doi.org/10.1016/j.egyr.2021.11.017

[20] S. yong LIU, C. long DU, X. xia CUI, Research on the cutting force of a pick. Min. Sci. Technol. (2009). DOI: https://doi.org/10.1016/S1674-5264(09)60096-X

[21] V. Raghavan, C.S.N. Murthy, Assessment and Prediction of Specific Energy Using Rock Brittleness in Rock Cutting. In: 2020. DOI: https://doi.org/10.1007/978-3-030-24314-2_46

[22] Q.Q. Zhang, Z.N. Han, M.Q. Zhang, J.G. Zhang, Experimental study of breakage mechanisms of rock induced by a pick and associated cutter spacing optimization. Yantu Lixue/Rock Soil Mech. (2016). DOI: https://doi.org/10.16285/j.rsm.2016.08.007

[23] J. Rojek, E. Oñate, C. Labra, H. Kargl, Discrete element simulation of rock cutting. Int. J. Rock Mech. Min. Sci. (2011). https://doi.org/10.1016/j.ijrmms.2011.06.003

[24] J. Huang, Y. Zhang, L. Zhu, T. Wang, Numerical simulation of rock cutting in deep mining conditions, Int. J. Rock Mech. Min. Sci. (2016). DOI: https://doi.org/10.1016/j.ijrmms.2016.02.003

[25] G. Van Wyk, D.N.J. Els, G. Akdogan, S.M. Bradshaw, N. Sacks, Discrete element simulation of tribological interactions in rock cutting. Int. J. Rock Mech. Min. Sci. (2014). DOI: https://doi.org/10.1016/j.ijrmms.2013.10.003

[26] X. Zhang, H. Jiang, H. Li, C. Gu, L. Zhao, Rock fragmentation using the disc tool assisted by the prefabricated kerf: Numerical modelling based on discrete element method (DEM). Eng. Fract. Mech. (2023). DOI: https://doi.org/10.1016/j.engfracmech.2023.109159

[27] H. Jiang, D. Meng, 3D numerical modelling of rock fracture with a hybrid finite and cohesive element method. Eng. Fract. Mech. (2018). DOI: https://doi.org/10.1016/j.engfracmech.2018.05.037

[28] Z. Wang, Q. Zeng, Z. Lu, L. Wan, X. Zhang, G. Gao, Numerical Simulation of Conical Pick Cutting Arc Rock Plate Fracture Based on ANSYS/LS-DYNA. Adv. Mater. Sci. Eng. (2020). DOI: https://doi.org/10.1155/2020/6563520

[29] Z. Lu, L. Wan, Q. Zeng, X. Zhang, K. Gao, Numerical Simulation of Rock Plate Cutting with Three Sides Fixed and One Side Free. Adv. Mater. Sci. Eng. (2018). DOI: https://doi.org/10.1155/2018/5464295

[30] H. Jeong, S. Choi, S. Lee, S. Jeon, Rock cutting simulation of point attack picks using the smooth particle hydrodynamics technique and the cumulative damage model. Appl. Sci. (2020). DOI: https://doi.org/10.3390/APP10155314

[31] H. Zhang, H. Ni, B. Huang, S. Liu, Y. Wang, H. Liang, X. Guo, Research on discrete element modeling and numerical simulation of cutting rock behavior under impact load. Energy Sci. Eng. (2022). DOI: https://doi.org/10.1002/ese3.1146

[32] O.K. Mahabadi, B.E. Cottrell, G. Grasselli, An example of realistic modelling of rock dynamics problems: FEM/DEM simulation of dynamic brazilian test on Barre Granite. Rock Mech. Rock Eng. (2010). DOI: https://doi.org/10.1007/s00603-010-0092-7

[33] Y. Li, C. Xia, Time-dependent tests on intact rocks in uniaxial compression. Int. J. Rock Mech. Min. Sci. (2000). DOI: https://doi.org/10.1016/S1365-1609(99)00073-8

[34] J.Y. Park, H. Kang, J.W. Lee, J.H. Kim, J.Y. Oh, J.W. Cho, J. Rostami, H.D. Kim, A study on rock cutting efficiency and structural stability of a point attack pick cutter by lab-scale linear cutting machine testing and finite element analysis. Int. J. Rock Mech. Min. Sci. (2018). hDOI: ttps://doi.org/10.1016/j.ijrmms.2018.01.034

[35] S.K. Palaniappan, S.K. Pal, M.P. Dikshit, A study on rock cutting forces and wear mechanisms of coated picks by lab-scale linear cutting machine. In: Springer Ser. Geomech. Geoengin. (2020). DOI: https://doi.org/10.1007/978-3-030-33954-8_53

[36] S. Feng Wang, Y. Tang, X. Bing Li, K. Du, Analyses and predictions of rock cuttabilities under different confining stresses and rock properties based on rock indentation tests by conical pick. Trans. Nonferrous Met. Soc. China (English Ed. (2021). DOI: https://doi.org/10.1016/S1003-6326(21)65615-7

[37] M. Entacher, J. Rostami, TBM performance prediction model with a linear base function and adjustment factors obtained from rock cutting and indentation tests. Tunn. Undergr. Sp. Technol. (2019). DOI: https://doi.org/10.1016/j.tust.2019.103085

[38] D. Huang, X. Wang, O. Su, Z. Jie Zheng, M. Gao, Study on the cuttability characteristics of granites under conical picks by indentation tests. Bull. Eng. Geol. Environ. (2022). DOI: https://doi.org/10.1007/s10064-022-02703-1

[39] S. Hojjati, H. Jeong, J.-W. Cho, D. Tumac, S. Jeon, A prediction model for specific energy required by point attack picks based on a hybrid evolutionary machine learning technique. Arab. J. Geosci. (2022). DOI: https://doi.org/10.1007/s12517-022-10225-z

[40] O. Su, N. Ali Akcin, Numerical simulation of rock cutting using the discrete element method. Int. J. Rock Mech. Min. Sci. (2011). DOI: https://doi.org/10.1016/j.ijrmms.2010.08.012

[41] E. Juhasz, R.M. Movahedi, I. Fekete, S. Fischer, Discrete element modelling of particle degardation of railway ballast material with PFC3D software. Sci. Transp. Progress. Bull. Dnipropetr. Natl. Univ. Railw. Transp. (2019). DOI: https://doi.org/10.15802/stp2019/194472

[42] Q.Q. Zhang, Z.N. Han, S.H. Ning, Q.Z. Liu, R.W. Guo, Numerical simulation of rock cutting in different cutting mode using the discrete element method. J. Geoengin. (2015). DOI: https://doi.org/10.6310/jog.2015.10(2).1

[43] J. Rostami, L. Ozdemir, D.M. Neil, Performance prediction: a key issue in mechanical hard rock mining. Min. Eng. (1994). DOI: https://doi.org/10.1016/0148-9062(95)97085-w